# Matrix Metalloproteinase 9 Facilitates West Nile Virus Entry into the Brain[▽]

Penghua Wang,[1] Jianfeng Dai,[1] Fengwei Bai,[1] Kok-Fai Kong,[2] Susan J. Wong,[4]
Ruth R. Montgomery,[2] Joseph A. Madri,[3] and Erol Fikrig[1]*

*Section of Infectious Diseases[1] and Section of Rheumatology,[2] Department of Internal Medicine, and Department of Pathology,[3]
Yale University School of Medicine, New Haven, Connecticut 06520, and Diagnostic Immunology Laboratory,
Wadsworth Center, New York State Department of Health, Albany, New York 12201[4]*

West Nile virus (WNV) is the most-common cause of mosquito-borne encephalitis in the United States. Invasion of the brain by WNV is influenced by viral and host factors, and the molecular mechanism underlying disruption of the blood-brain barrier is likely multifactorial. Here we show that matrix metalloproteinase 9 (MMP9) is involved in WNV entry into the brain by enhancing blood-brain barrier permeability. Murine MMP9 expression was induced in the circulation shortly after WNV infection, and the protein levels remained high even when viremia subsided. In the murine brain, MMP9 expression and its enzymatic activity were upregulated and MMP9 was shown to partly localize to the blood vessels. Interestingly, we also found that cerebrospinal fluid from patients suffering from WNV contained increased MMP9 levels. The peripheral viremia and expression of host cytokines were not altered in $MMP9^{-/-}$ mice; however, these animals were protected from lethal WNV challenge. The resistance of $MMP9^{-/-}$ mice to WNV infection correlated with an intact blood-brain barrier since immunoglobulin G, Evans blue leakage into brain, and type IV collagen degradation were markedly reduced in the $MMP9^{-/-}$ mice compared with their levels in controls. Consistent with this, the brain viral loads, selected inflammatory cytokines, and leukocyte infiltrates were significantly reduced in the $MMP9^{-/-}$ mice compared to their levels in wild-type mice. These data suggest that MMP9 plays a role in mediating WNV entry into the central nervous system and that strategies to interrupt this process may influence the course of West Nile encephalitis.

Mosquito-borne flaviviruses are emerging as increasing threats to human health. For example, West Nile virus (WNV) is maintained worldwide in an enzootic cycle between the avian hosts and mosquito vectors. Since the outbreak in New York City in 1999, WNV has rapidly spread throughout North America, resulting in over 20,000 human cases through 2006, with a mortality rate of 3.9% (11). Infection is often asymptomatic, but high fever, meningitis, encephalitis, or acute flaccid paralysis may occur in 20 to 40% of infected individuals (11). Encephalitis is the major cause of death and is most common in the elderly (Centers for Disease Control and Prevention, Atlanta, GA).

The mechanisms by which neurotropic flaviviruses enter the central nervous system (CNS) are not well understood. In theory, WNV can enter the brain through multiple pathways, including endothelial tight junctions, direct infection of endothelial cells, infected leukocytes that traffic to the CNS, infection of olfactory neurons, and/or direct axonal retrograde transport from infected peripheral neurons (7, 27, 28). It has recently been shown that increased peripheral viremia in Toll-like receptor 3 (TLR3)-deficient mice ($TLR3^{-/-}$) did not result in increased viral entry into the brain. In contrast, $TLR3^{-/-}$ mice were resistant to lethal WNV challenge owing to better blood-brain barrier (BBB) integrity (30), suggesting that WNV enters the brain primarily through the BBB. The

mechanisms by which WNV crosses the BBB, as well as the host factors that mediate viral entry, have not yet been fully elucidated. The BBB is comprised of several layers: the tight endothelium formed by endothelial cells through tight junctions and the basement membrane composed of mainly type IV collagen, laminin, proteoglycan, several glycoproteins (21), and astroglial end feet. The opening of the BBB and retraction of glial end feet are characterized by the loss of tight junctions and degradation of basement membranes, which is catalyzed in part by matrix metalloproteinases (MMPs) (20, 24). MMPs are traditionally considered responsible for the turnover of extracellular matrix (ECM), but recently they have been shown to function in innate immunity and inflammation, probably by modulating cytokine/chemokine activity and other proteins (22). In response to cytokines, MMPs, together with a number of potent chemokines, play an important role in orchestrating leukocyte extravasation into the inflammatory focus. Indeed, of the major MMPs controlling the basement membrane turnover and tight-junction efficiency, MMP2 and -9 have been shown to enhance leukocyte infiltration into the CNS in an experimental autoimmune encephalomyelitis model (1, 8, 10), to facilitate the pulmonary infection and pathogenesis of an intracellular bacterium, *Francisella tularensis* (17), and to induce vascular leakage in a Dengue virus infection model (15).

The molecular mechanisms underlying CNS invasion by neurotropic flaviviruses are awaiting characterization. The murine model has been well established for the study of the pathogenesis of WNV encephalitis (27). In this study, we try to understand how WNV crosses the BBB, a key step leading to lethal encephalitis in the mouse model. Identifying molecules mediating viral entry into the CNS may lead to

---

* Corresponding author. Mailing address: Section of Infectious Diseases, Department of Internal Medicine, Yale University School of Medicine, The Anlyan Center for Medical Research Room S525A, 300 Cedar Street, New Haven, CT 06520-8031. Phone: (203) 785-2453. Fax: (203) 785-3864. E-mail: erol.fikrig@yale.edu.

new strategies to prevent, or reduce, the mortality resulting from encephalitis.

## MATERIALS AND METHODS

**Animal and human studies.** The murine study was reviewed and approved by the Yale University Institutional Animal Care and Use Committee. Five- to 6-week-old FVB/NJ and MMP9 knockout mice (stock no. 004104; $MMP9^{-/-}$) from JAX Mice and Services (Bar Harbor, ME) were used throughout the study unless otherwise specified. As the $MMP9^{-/-}$ mice were made on the B6/129S background and backcrossed to FVB/NJ for five generations to exclude the potential cofounding effects of B6/129S, a congenic analysis was performed by testing $MMP9^{-/-}$ mice with a 100-marker panel that distinguishes between FVB and B6/129. The microsatellite markers were spread across the 19 autosomes and the X chromosome at approximately 15-centimorgan intervals. The results showed that, excluding the MMP9 region, $MMP9^{-/-}$ mice shared 94.6% identity with FVB/NJ. Cerebrospinal fluid (CSF) samples from patients suffering from WNV acute infection were provided by the Diagnostic Immunology Laboratory of the Wadsworth Center (New York State Department of Health). All spinal fluids were tested by immunoglobulin M (IgM) capture enzyme-linked immunosorbent assay (ELISA) according to a method described by Martin et al. (18). Reagents were provided by the CDC (Ft. Collins, CO) and by the National Microbiology Laboratory of the Public Health Agency of Canada (Winnipeg, Manitoba, Canada). Paired sera from the patients with spinal fluids positive by IgM capture ELISA were tested by cross-species plaque reduction neutralization tests that included WNV and St. Louis encephalitis virus according to the method described by Lindsey et al. (13). But only some CSF samples from these patients were positive for WNV as determined by reverse transcription-PCR (RT-PCR). Whether the CSF samples were positive or negative for WNV ($n$ = 7/group) was determined by quantitative RT-PCR using the envelope gene primers and probe. Samples were obtained following protocols approved by New York State. All samples were preexisting and obtained before this study was initiated.

**Quantitative PCR.** Selected MMPs or tissue inhibitors of MMPs (TIMPs) were further quantified by RT-PCR. Custom-designed Taqman primers and probes were purchased from Applied Biosystems (Foster City, CA). All these custom-made oligonucleotides were optimized and quality assured by the service provider. PCR conditions were 50°C for 2 min, 95°C for 10 min, 40 cycles of 95°C for 15 s, and 60°C for 30 s. Changes in the levels of the gene transcripts were calculated by using the threshold cycle method.

**Culture of PBMCs.** Peripheral blood mononuclear cells (PBMCs) were isolated from freshly heparinized blood from healthy donors and plated into a six-well plate. Nonadherent cells were washed off after being incubated in a $CO_2$ incubator at 37°C for 2 hours. The attached cells were further cultured for 7 days in RPMI 1640 medium supplemented with 20% human sera (Cambrex, North Brunswick, NJ). Cells were washed once with prewarmed fresh medium and then infected with WNV at a multiplicity of infection (MOI) of 1 for 1, 24, 48, and 72 h.

**ELISA.** Protein levels in mouse sera were quantified by ELISA (R&D, Minneapolis, MN). Briefly, capture-monoclonal anti-MMP9/TIMP-1 was precoated into a 96-well plate and blocked with 200 μl of 5% skim milk at room temperature (unless specified, all steps were performed at room temperature) for 1 h. After plates were washed, 100 μl of properly diluted samples was added to each well and incubated for 1 h. After plates were washed, 100 μl of biotin-labeled anti-MMP9 was added and incubated for 1 h. Then, 100 μl of avidin-horseradish peroxidase (HRP) was added and incubated for 30 min. After a stringency wash, 100 μl of substrate was added to each well, the color was developed for 15 to 30 min, and the optical density at 450 nm was finally read by using a plate reader.

**Zymography.** To test the enzymatic activity of MMP9, we performed zymography as described previously (1). Briefly, brain lysate was resolved on a 7.5% nonreducing sodium dodecyl sulfate-polyacrylamide gel electrophoresis (SDS-PAGE) gel containing 0.4% gelatin. The gel was washed with 50 mM Tris-HCl, pH 7.5, containing 2.5% Triton X-100 for 2 h at room temperature and incubated overnight in 50 mM Tris-HCl, pH 7.5, containing 10 mM $CaCl_2$, 1 μM $ZnCl_2$ at 37°C. Protein bands were visualized by Coomassie blue staining followed by destaining.

**Mouse infection.** MMP9 knockout mice, together with the corresponding wild type (5 to 6 weeks, FVB/NJ; JAX Mice and Services, Bar Harbor, ME), were infected intraperitoneally with 500 PFU of WNV isolate 2741 in 100 μl of 1× phosphate-buffered saline (PBS) containing 5% gelatin.

**Quantification of viremia and cytokines in the blood/brain.** Total RNA was extracted from whole blood or brains by using a Qiagen kit. Standard quantitative RT-PCR was performed to quantify WNV viral loads or cytokine mRNA.

## TABLE 1. Primers and probes[a]

| Gene product | Sequence |
| --- | --- |
| *M. musculus* Mmp9 | F: 5-TGGACGCGACCGTAGTTG-3<br>R: 5-GCTTGCCCAGGAAGACGAA-3<br>P: 5-6FAM-CTGTGCGTCTTCCCC-MGB-3 |
| *M. musculus* Mmp2 | F: 5-GAGACCGCTATGTCCACTGT-3<br>R: 5-CTTGTTGCCCAGGAAAGTGAAG-3<br>P: 5-6FAM-CACCTTCTGAATTTCC-MGB-3 |
| *M. musculus* β-actin | F: 5-AGAGGGAAATCGTGCGTGAC-3<br>R: 5-CAATAGTGATGATGACCTGGCCGT-3<br>P: 5-6FAM-CACTGCCGCATCCTCTTCCTCCC-TAMRA-3 |
| *M. musculus* TNF-α | F: 5-CTCCAGGCGGTGCCTATGT-3<br>R: 5-GAAGAGCGTGGTGGCCC-3<br>P: 5-6FAM-CAGCCTCTTCTCATTCCTGCTTGTGGC-TAMRA-3 |
| *M. musculus* IL-6 | F: 5-CCAGAAACCGCTATGAAGTTCC-3<br>R: 5-TCACCAGCATCAGTCCCAAG-3<br>P: 5-6FAM-TCTGCAAGAGACTTCCATCCAGTTGCCT-TAMRA-3 |
| *M. musculus* IFN-α | F: 5-CTTCCACAGGATCACTGTGTACCT-3<br>R: 5-TTCTGCTCTGACCACCTCCC-3<br>P: 5-6FAM-AGAGGAGAAGAAACACAGCCCCTGTGCC-TAMRA-3 |
| WNV E | F: 5-TTCTCGAAGGCGACAGCTG-3<br>R: 5-CCGCCTCCATATTCATCATC-3<br>P: 5-6FAM-ATGTCTAAGGACAAGCCTACCATC-TAMRA-3 |

[a] Primers and probes for *Homo sapiens* MMP2, MMP9, and TIMP-2 and *M. musculus* MMP3, MMP13, TIMP-1, and TIMP-2 are inventoried products of Applied Biosystems. F, forward; R, reverse; P, probe; 6FAM, 6-carboxyfluorescein; TAMRA, 6-carboxytetramethylrhodamine; MGB, minor groove binding.

Primers and probes for specific cytokines have been well established in our laboratory (30) and can be found in Table 1.

**Western blotting.** Brain tissues were resuspended in sample buffer, without boiling, and 2-mercaptomethanol; cleared by centrifugation at $20,000 \times g$; and resolved on a 4- to 15%-gradient SDS-PAGE gel. Antigens were probed with specific antibodies, followed by HRP-conjugated secondary antiserum, and detected with an enhanced chemilumiscence system from GE Healthcare Bio-Sciences Corp. (Piscataway, NJ). Rabbit anti–mouse type IV collagen and β-actin were obtained from Santa Cruz Biotechnology, Inc. (Santa Cruz, CA).

**BBB permeability.** The BBB permeability of WNV in infected wild-type mice and MMP9 knockouts was assessed at day 4 postinfection. Mice were injected intraperitoneally with 800 μl of 1% (wt/vol) Evans blue dye and, 1 h later, perfused with PBS until the drainage was colorless. Well-perfused brain was free of blood. For quantification of Evans blue, whole brains were fixed with 4% paraformaldehyde and ground to fine powder in liquid nitrogen. The powder was washed with 2 ml of PBS and then resuspended in 1 ml of dimethyl sulfoxide (DMSO) by vortexing. After being centrifuged at $13,000 \times g$ for 10 min, the supernatants (DMSO extracts) were removed carefully and the absorbance at a wavelength of 611 nm was measured by using a spectrometer. A DMSO extract from a clean mouse brain was used as a blank.

**Histology, immunofluorescence microscopy, and IHC.** Mice were transcardially perfused with ice-cold PBS, and brains were fixed in 4% paraformaldehyde overnight at 4°C. Brains were either cryosectioned or sectioned in paraffin. For immunohistochemistry (IHC), paraffin sections were deparaffinized; rehydrated with 100% xylene, 95% ethanol; and blocked with 3% $H_2O_2$ in methanol for 10 min. Sections were treated with Retrievagen A (BD Biosciences) for 10 min at 95°C and blocked with 10% goat serum in PBS for 1 h. Specific antibodies were applied to sections, followed by biotinylated secondary antibody and streptavidin-conjugated HRP. Sections were finally developed using diaminobenzidine chromogen. For immunofluorescence assay of cryosections, sections were fixed with 4% paraformaldehyde for 20 min and permeabilized with 0.5% Triton X-100 in PBS for 15 min. Sections were stained with specific antibodies, followed by fluorophore-labeled secondary antibody. Images were acquired by using a Zeiss fluorescence microscope. Rat anti-CD45 was purchased from BD Biosciences (Franklin Lakes, NJ), rat anti-mouse MMP9 from R&D Systems (Min-
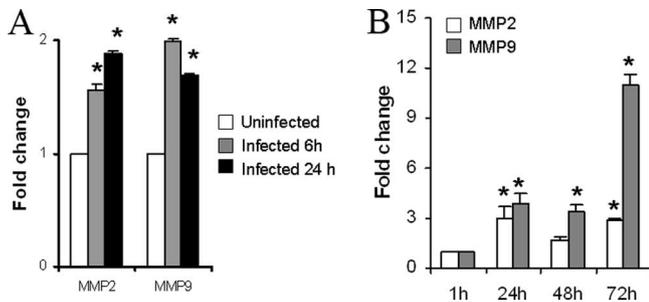
FIG. 1. MMP2 and -9 expression in macrophages. (A) Peritoneal macrophages from mice were infected with WNV (MOI = 1) for 6 and 24 h. Total RNA was purified and converted into cDNA, and selected transcripts were assessed by quantitative RT-PCR. Bars represent the changes in the levels in infected samples compared to the levels in uninfected controls. Data shown represent the results of one of three experiments with similar results. ∗, $P < 0.01$. (B) Expression of MMP2 and -9 in human macrophages. Amounts of $1 \times 10^6$ PBMCs were isolated from fresh blood and grown in vitro for 7 days. Cells were infected with WNV (MOI = 1) for the indicated time intervals. Data represent the means ± standard errors of the pooled results ($n = 5$). ∗, $P$ values were between <0.05 and 0.0001.

neapolis, MN), and rabbit anti-WNV-envelope E protein from Abcam, Inc. (Cambridge, MA). Hematoxylin-and-eosin (H&E)-stained sections were scored from 0 to 3, with 3 being the most-severe brain pathology based on the numbers of perivascular leukocytes, microglial nodules, and variable necrosis (11).

**Graphs and statistics.** Survival curves and statistical analyses were produced by using PRISM 4 software (Graphpad Software, San Diego, CA). Other statistical analysis used either the Mann-Whitney U test, where specified, or the unpaired two-tailed Student's $t$ test, with a cutoff $P$ value of 0.05.

## RESULTS

**Gelatinase expression is elevated in response to WNV challenge in vitro.** The MMPs are a family of proteinases with at least 24 members in mice. To determine which MMPs are induced by WNV, we performed microarrays with mRNA from murine peritoneal macrophages infected with WNV for 24 h. MMP2 and -9 were induced, and all TIMPs were downregulated in the phagocytes in response to WNV (data not shown). MMP2 and -9 are type IV collagenases that cleave type IV collagen in the basement membranes that comprise the BBB. We further assessed the microarray data by quantitative PCR. As seen in Fig. 1A, MMP2 and MMP9 were significantly upregulated, by 1.5- to 2-fold ($P < 0.01$), consistent with the array data. To extend these results to humans, we quantified MMP2 and MMP9 mRNA from five healthy individuals. PBMCs were isolated, cultured for 7 days, and infected with WNV. As shown in Fig. 1B, relative to the levels 1 h postinfection, the MMP2 and 9 levels at 24, 48, and 72 h postinfection were significantly increased ($P$, <0.05 to 0.0001), with MMP9 being the mostly markedly elevated.

**MMP9 activity is preferentially induced by WNV in vivo.** We next examined the expression profiles of MMP2 and -9 during the course of WNV infection in vivo. When whole-blood viremia was evident in the circulation from day 1 to 2, MMP9 mRNA levels also increased, and when the viremia receded at day 5, the MMP9 mRNA levels also decreased (Fig. 2A and B). MMP9 protein levels in the sera went up steadily through day 5 (Fig. 2C). Our results also indicate that MMP9 expression in all individuals was induced upon WNV challenge, but the lev-
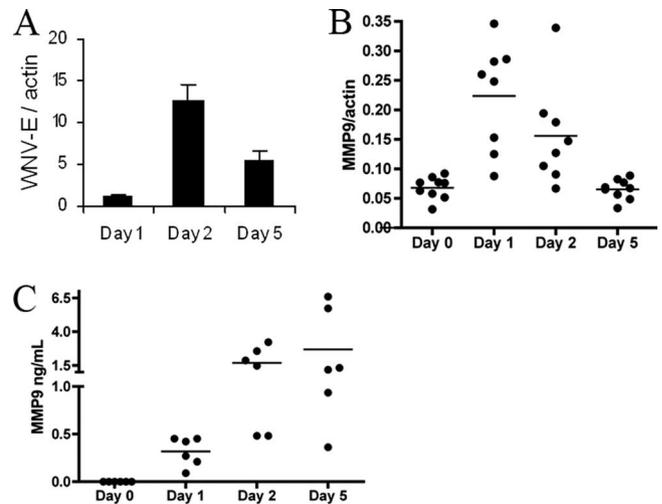


FIG. 2. MMP9 in the blood of WNV-infected mice. Wild-type mice ($n = 8$) were infected with 500 PFU of WNV, and whole-blood samples were drawn at the indicated time points. Levels of WNV E (A) and MMP9 (B) gene expression in the whole blood were assessed by quantitative RT-PCR. Bars represent the means ± standard errors of the results. MMP9 transcripts were significant higher at days 1 and 2 than at day 0 ($P < 0.001$). (C) MMP9 protein levels in the sera were quantified by ELISA. MMP9 levels were significantly elevated at days 2 and 5 compared to the levels on day 0 ($P < 0.01$). Horizontal lines, means of results.

els of induction varied significantly between individuals. However, the MMP2 mRNA level remained unchanged upon WNV infection through day 5 (data not shown), reflecting the fact that MMP2 is constitutively expressed in vivo (22).

In this study, we focused on MMP9 because its expression and activity are highly inducible (26) and it was the most-highly influenced by WNV infection. In the murine brain, MMP9 was upregulated by WNV at mRNA and protein levels. Coincident with the brain viral load, MMP9 mRNA levels increased by fivefold at day 5 compared to the levels at day 0 (Fig. 3A and B). By zymography, MMP9 gelatinase activity was evident in the infected brains at day 7, while it was not detected in uninfected wild-type or infected $MMP9^{-/-}$ mouse brains. MMP2 gelatinase activity was observed in all brain samples, albeit at much lower levels than MMP9 activity (Fig. 3C). This suggests that WNV mainly induces MMP9 gelatinase activity in the brain. We also examined the localization of MMP9 in the brains infected with WNV at various time points (Fig. 3D). Uninfected (day 0) mouse brain blood microvessels expressed low levels of MMP9. At day 3, when viremia was evident, MMP9 expression was also highly induced in blood microvascular endothelia and infiltrating leukocytes (Fig. 3D). Subsequently, following virus entry and spread in the brain at days 5 and 7, more and much brighter MMP9 staining was noted in brain parenchyma (Fig. 3D). This indicates that MMP9 expression by the BBB preceded virus entry into the CNS and that the presence of WNV in the CNS upregulated the expression of MMP9 by infiltrating not only leukocytes but also brain-resident cells. We also obtained CSF samples from patients with acute, early WNV infection as determined by IgM capture ELISA and by neutralization tests of the sera. Some of the CSF samples from these patients were positive for WNV as deter-
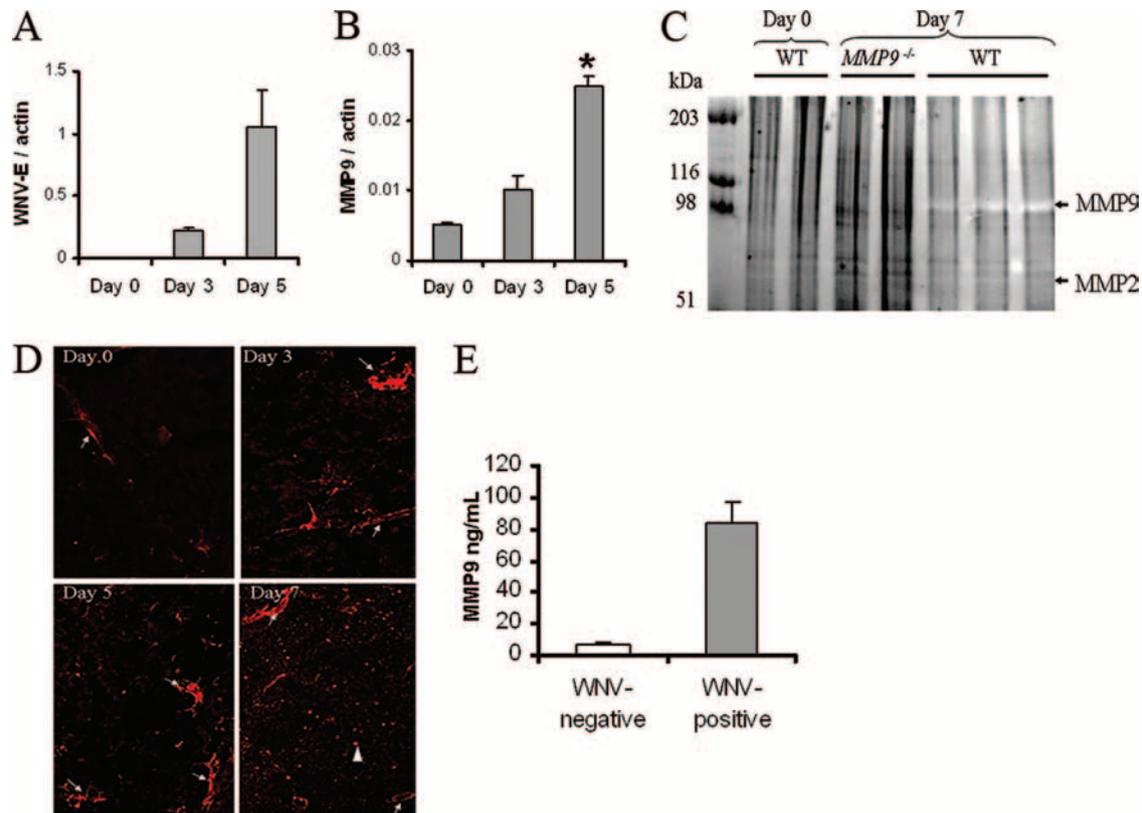
FIG. 3. MMP9 expression in the brains of WNV-infected mice and the CSF of WNV patients. Wild-type mice were infected with 500 PFU of WNV and perfused with PBS at days 3, 5, and 7 postinfection. WNV E (A) and MMP9 (B) transcripts were examined by quantitative RT-PCR. Bars represent the means ± standard errors of the results ($n = 5$ for each time point). (C) Zymography results. The transparent bands indicate the presence of gelatinase, MMP9, or MMP2. WT, wild type. (D) Localization of MMP9. Infected mice were sacrificed and perfused at days 0, 3, 5, and 7. Brain sections (cerebral cortex) were stained for MMP9. Images were acquired by using a Zeiss AxioCam fluorescence microscope. Original magnification is ×100. Arrows indicate MMP9 staining on blood vessels, and arrowheads point to MMP9 staining in brain parenchyma. (E) Total MMP9 levels in the WNV-negative and -positive CSF samples were determined by ELISA ($n = 7$/group). Bars represent the means ± standard errors of the results. ∗, $P < 0.04$.

mined by RT-PCR. We found that the MMP9 protein levels in the WNV-positive CSF increased dramatically compared to the levels in the WNV-negative CSF (Fig. 3E).

**Characterization of $MMP9^{-/-}$ mice challenged with WNV.** To investigate the physiological relevance of elevated MMP9 activity in the pathogenesis of WNV encephalitis, we challenged mice with WNV and compared the survival rates of $MMP9^{-/-}$ and wild-type animals. As seen in Fig. 4A, $MMP9^{-/-}$ mice had an increased survival rate compared with that of wild-type animals ($P < 0.04$; $n = 27$/group), even though the peripheral viremia and virus titers were similar in both groups of mice (Fig. 4B). To determine whether cytokine expression was altered in $MMP9^{-/-}$ mice, the transcript levels of selected cytokines in the periphery were analyzed by quantitative RT-PCR. No significant differences between wild-type and $MMP9^{-/-}$ mice were observed for levels of interleukin-6 (IL-6) and tumor necrosis factor alpha (TNF-α) (Fig. 4C and D), proinflammatory cytokines that are highly responsive to WNV infection. As brain invasion by WNV is a critical step in the pathogenesis of encephalitis, we determined whether the resistance of $MMP9^{-/-}$ mice is due to reduced viral entry into the brain. We measured the brain viral loads at days 5 and 7 postinfection and found that $MMP9^{-/-}$ mice harbored a sig-

nificantly lower viral load than control mice at day 7 (Fig. 5A and B). Consistent with this, the expression of selected cytokines, including alpha interferon, TNF-α, and IL-6 (Fig. 5C to E), was also decreased in the $MMP9^{-/-}$ mouse brains. We then examined CD45$^+$ cells, including leukocyte infiltrates and microglia in the cerebral cortex. As shown in Fig. 5F, wild-type mouse tissue had more CD45$^+$ cells than $MMP9^{-/-}$ mouse tissue, which correlates with the higher virus loads and degree of inflammation in wild-type mouse tissue. The results of H&E staining also showed that in the cerebral cortex, wild-type tissue had increased infiltration of leukocytes, neurons with condensed and aggregated nuclear chromatin, and microglial nodules formed by clusters of microglial/infiltrating cells around necrotic brain tissues in comparison to these characteristics in the $MMP9^{-/-}$ mice (Fig. 5G). H&E-stained sections were scored based on the numbers of perivascular leukocytes, microglial nodules, and sick neurons (11). The mean score for the wild-type mice was 2.1 ± 0.08 (mean ± standard error of the mean) versus 1.3 ± 0.09 for the mutants ($n = 10$). These data suggest that MMP9 plays a role in mediating WNV entry into the brain.

**MMP9 facilitates WNV entry into the brain by disrupting the BBB.** As a proteinase, MMP9 has been shown to cleave not
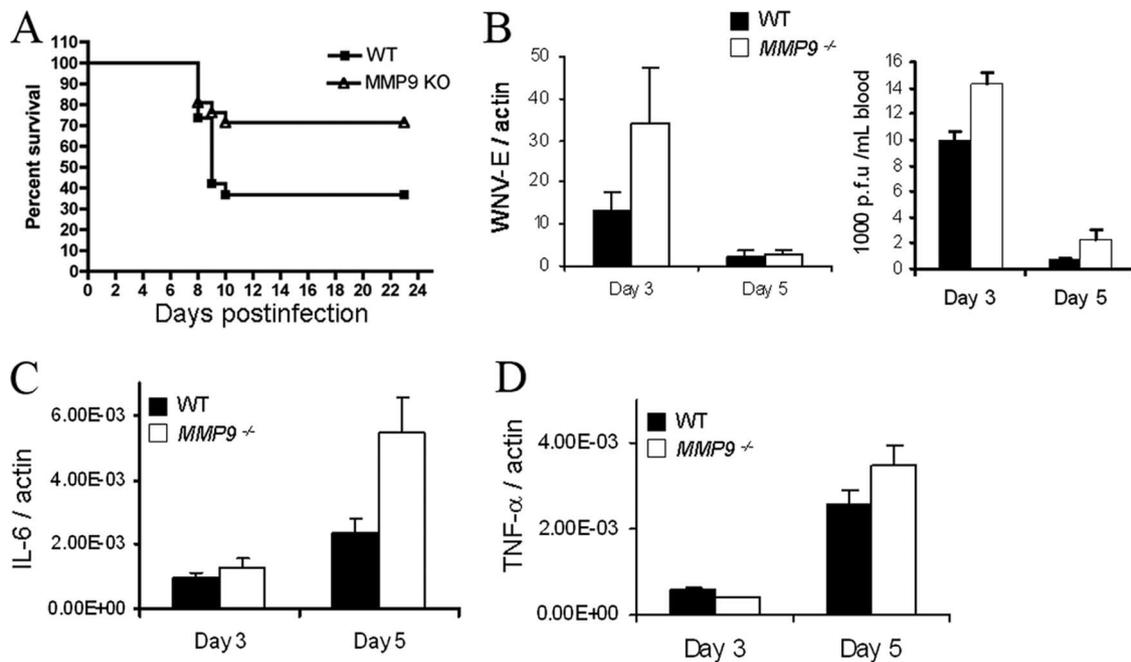
FIG. 4. Phenotypic analyses of $MMP9^{-/-}$ mice upon WNV infection. (A) Wild-type and $MMP9^{-/-}$ mice were infected with 500 PFU of WNV and monitored for mortality daily. Data are pooled from the results of two experiments ($n = 27$/group). $P < 0.04$. (B) Viremia in the whole blood at selected time points (left panel) was examined by quantitative RT-PCR using the WNV E gene and normalized with murine actin ($n = 10$/group). Virus titers in sera were determined by plaque assay and are expressed as PFU per ml of sera (right panel). Bars indicate the means ± standard errors of the results from two experiments ($n = 10$/group). Blood IL-6 (C) and TNF-α (D) levels were examined by using quantitative RT-PCR. Bars represent the means ± standard errors of the results from two experiments ($n = 10$/group). WT, wild type; KO, knockout.

only type IV collagen, the major component of basement membranes (~50% of all basement membrane proteins) of the BBB, but also other components of the brain endothelial ECM. To evaluate whether MMP9 contributes to the disruption of the BBB during WNV infection, we examined Evans blue and IgG leakage into the brain at day 4 and 7, respectively. The results shown in Fig. 6A indicate that IgG levels in the perfused brains of the $MMP9^{-/-}$ mice were decreased in comparison to those in infected wild-type mice, suggesting that MMP9 modulates BBB permeability during WNV infection. Furthermore, leakage of Evans blue into the perfused brain of $MMP9^{-/-}$ mice was less than in controls (Fig. 6C and D). In addition, type IV collagen in the infected wild-type mice was hardly detected, while it was evident in uninfected mice or infected $MMP9^{-/-}$ mice (Fig. 6A and B). This suggests that WNV infection results in loss of collagen IV mainly through the collagenase activity of MMP9. Finally, to further confirm that reduced viral loads in the brain and enhanced survival of $MMP9^{-/-}$ mice were attributable to decreased WNV neuroinvasion, WNV was inoculated intracerebrally, and no significant difference in survival rates was noted between wild-type and $MMP9^{-/-}$ mice (data not shown). These data collectively suggest that MMP9 facilitates WNV entry into the brain by disrupting the BBB.

## DISCUSSION

Viral invasion of the brain is a critical step in the pathogenesis of diseases following the dissemination of virus in the periphery. Although it is clear that both viral and host factors

are involved, the molecular mechanisms underlying brain penetration by neurotropic flaviviruses, such as WNV, Japanese encephalitis virus, and Murray Valley encephalitis virus, are not clearly understood. We show that MMP9 facilitates WNV entry into the brain by enhancing BBB permeability. Several lines of evidence support this conclusion. First, MMP9 is upregulated upon WNV infection both in the periphery and brain, and it is partly localized to the brain blood vessels. Second, mice without MMP9 have equivalent levels of peripheral viremia but are more resistant to lethal challenge with WNV than the wild type. In addition, $MMP9^{-/-}$ mice infected with WNV have a lower viral load and diminished leukocyte infiltrates, inflammatory cytokines, and neuronal damage in the brain compared to the wild type. Third, in the absence of MMP9, Evans blue and IgG leakage into the brain is reduced. Lastly, collagen IV, the major component of BBB basement membranes, is better retained in $MMP9^{-/-}$ mice during WNV infection.

It is believed that the potential of certain blood-borne viruses to invade the CNS is positively correlated with their ability to generate a high level of viremia (3). In mice, WNV replicates quickly in the peripheral tissues, with the highest level of viremia at days 3 to 4 postinfection, and is then cleared as adaptive immunity develops (6). During peak viremia, WNV begins to invade the brain, and the CNS viral load is evident at day 5 (30). Thus, the time window for WNV entry into the brain is narrow and WNV needs to get in efficiently. Invasion of the brain by WNV may take many paths, one of which, the BBB, is an important route for WNV, as has been supported by the results of previous studies (30, 16). However, the molecular
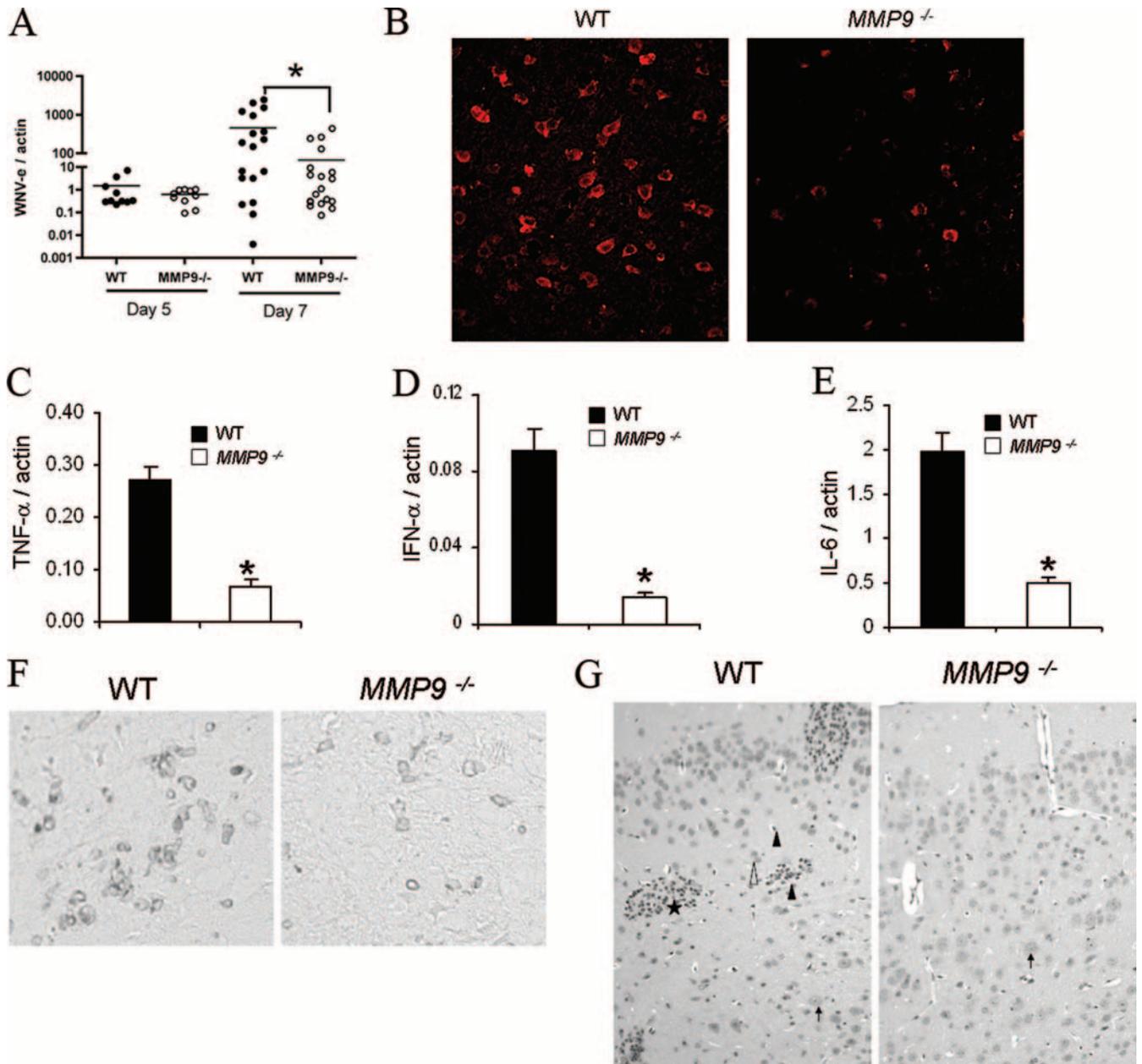
FIG. 5. Brain viral loads and histopathology of $MMP9^{-/-}$ mice infected with WNV. Wild-type and $MMP9^{-/-}$ mice were infected with 500 PFU of WNV for 5 and 7 days, euthanized, and perfused. (A) RNA was extracted from brains, and quantitative RT-PCR was performed to measure the transcripts of WNV E at days 5 and 7. *, P value of <0.04 by Mann-Whitney test. Horizontal lines, means of results. (C to E) The transcripts of TNF-α (C), alpha interferon (D), and IL-6 (E) in the brain at day 7 were measured by quantitative RT-PCR. Bars indicate the means ± standard errors of pooled results from two experiments (n = 10/group). *, P value of <0.04 by Mann-Whitney test. (B, F, and G) Results of immunofluorescence staining of WNV E (B), staining of CD45 by IHC (F), and H&E staining of cerebral cortex sections (G). Open triangle, neurons with condensed and aggregated nuclear chromatin; arrow, healthy neuron; closed triangle, infiltrating leukocytes; star, microglial nodules formed by clusters of microglial/infiltrating cells around necrotic brain tissues. All images were acquired by using a Zeiss AxioCam fluorescence microscope at a magnification of ×100. Shown are representative cerebral cortex sections from 10 mice/group. WT, wild type.

mechanisms underlying BBB permeability induced by WNV are not clear. By degrading ECM molecules, MMPs have been recognized to modulate blood vessel permeability during many biological processes, such as leukocyte extravasation and tumor metastasis (4, 9, 22, 25, 32). WNV may be carried in the infected leukocytes through the BBB into the brain with the aid of MMP activity. Through modulation of the basement membranes of the BBB, MMP2 and MMP9 derived from macrophages are crucial for leukocyte infiltration into brain in experimental autoimmunity encephalomyelitis (1). The predominant production of MMP9 by macrophages and T cells (12, 31) during viral infections may promote leukocyte extravasations in order to curb virus propagation. However, the influx of leukocytes that can support efficient virus replication may
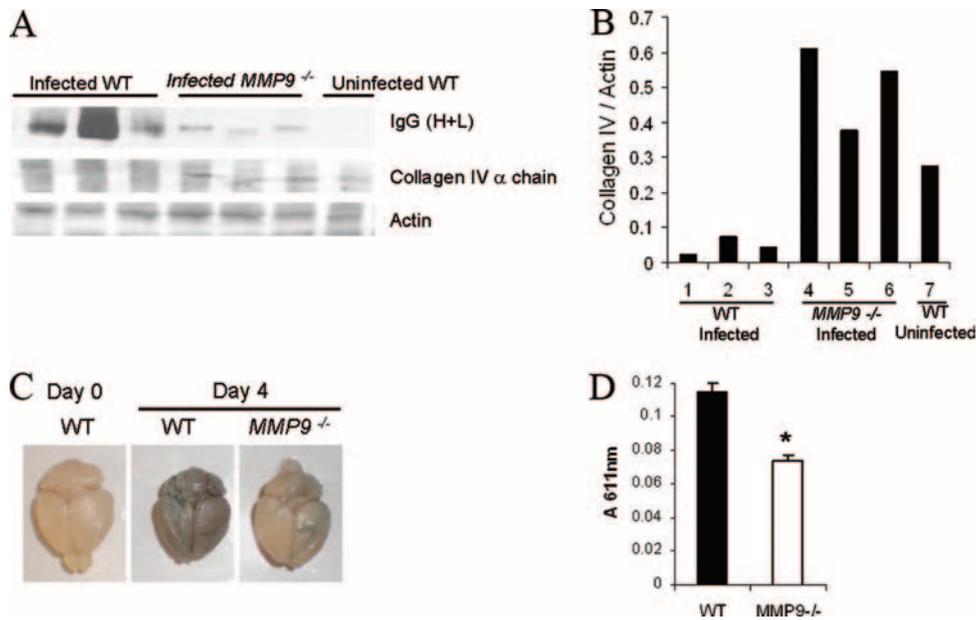
FIG. 6. BBB permeability in $MMP9^{-/-}$ mice infected with WNV. (A) Wild-type and $MMP9^{-/-}$ mice were infected with 500 PFU of WNV for 7 days, euthanized, and perfused. Brain samples (nondenatured) were resolved by SDS-PAGE, and Western blotting was performed to detect IgGs (~150 kDa), type IV collagen alpha chain (~160 kDa), and β-actin by using specific antibodies. (B) The intensities of type IV collagen bands were quantified and normalized with actin. Representative data from 3 out of 10 mice are shown here. (C) Wild-type and $MMP9^{-/-}$ mice were infected with 500 PFU of WNV and at day 4 injected with Evans blue and perfused 1 h later. Data are representative of the results of two experiments ($n$ = 10/group). (D) Quantification of Evans blue in the mouse brain. Evans blue was extracted from whole brains, and absorbance at a wavelength of 611 nm (A611 nm) was measured, using uninfected-mouse brain extract as a blank. Bars represent the means ± standard errors of the results ($n$ = 10/group). ∗, $P < 0.04$. WT, wild type.

actually carry viruses into the brain (2, 23, 30). In favor of this notion, knockout of ICAM-1, a receptor for leukocytes to traverse the endothelium, reduced the CNS viral load without affecting peripheral viremia (5). By reducing BBB permeability, viral influx is decreased to a level that resident microglia can then eradicate, and in the meantime, neuronal damage caused by the immune response is alleviated.

It is also possible that WNV crosses the endothelial layer by itself through leaky tight junctions or by transcytosis, like Japanese encephalitis virus (14), but it probably needs MMP9 to penetrate basement membranes. In both scenarios, MMP9 may play a role in facilitating WNV entry into the brain by enhancing BBB permeability (29). However, given that there is no apparent change in brain viral loads at day 5 when the BBB is opening (Fig. 5A), the possibility that BBB permeability per se is not directly linked to the virologic phenotype in the $MMP9^{-/-}$ mice could not be ruled out. Additionally, loss of the ECM resulting from excessive enzymatic activity of MMPs during viral infections is detrimental to brain neurons (24). In this sense, MMP9 expressed by brain-resident cells or infiltrates may exacerbate the detrimental effect of WNV infection in the brain. Although our efforts and the results of other studies (5, 30) cannot rule out other possible means of transport, including retrograde axonal transport (19, 28), that may be employed by WNV to enter the CNS, the BBB seems to contribute to WNV entry into the brain directly or in a "Trojan horse" manner (5, 16, 30).

In summary, we demonstrate that MMP9 is involved in the pathogenesis of WNV infection. The results of our study further the understanding of the molecular mechanisms underlying brain invasion by WNV, a key step in the pathogenesis of lethal encephalitis, and could offer a new strategy to reduce mortality.

## REFERENCES

1. **Agrawal, S., P. Anderson, M. Durbeej, N. van Rooijen, F. Ivars, G. Opdenakker, and L. M. Sorokin.** 2006. Dystroglycan is selectively cleaved at the parenchymal basement membrane at sites of leukocyte extravasation in experimental autoimmune encephalomyelitis. J. Exp. Med. **203:**1007–1019.
2. **Berger, J. R., and M. Avison.** 2004. The blood brain barrier in HIV infection. Front. Biosci. **9:**2680–2685.
3. **Chambers, T. J., and M. S. Diamond.** 2003. Pathogenesis of flavivirus encephalitis. Adv. Virus Res. **60:**273–342.
4. **Coussens, L. M., B. Fingleton, and L. M. Matrisian.** 2002. Matrix metalloproteinase inhibitors and cancer: trials and tribulations. Science **295:**2387–2392.
5. **Dai, J., P. Wang, F. Bai, T. Town, and E. Fikrig.** 2008. ICAM-1 participates in the entry of West Nile virus into the central nervous system. J. Virol. **82:**4164–4168.
6. **Diamond, M. S., B. Shrestha, A. Marri, D. Mahan, and M. Engle.** 2003. B cells and antibody play critical roles in the immediate defense of disseminated infection by West Nile encephalitis virus. J. Virol. **77:**2578–2586.
7. **Diamond, M. S., and R. S. Klein.** 2004. West Nile virus: crossing the blood-brain barrier. Nat. Med. **10:**1294–1295.
8. **Esparza, J., M. Kruse, J. Lee, M. Michaud, and J. A. Madri.** 2004. MMP-2 null mice exhibit an early onset and severe experimental autoimmune encephalomyelitis due to an increase in MMP-9 expression and activity. FASEB J. **18:**1682–1691.
9. **Goetzl, E. J., M. J. Banda, and D. Leppert.** 1996. Matrix metalloproteinases in immunity. J. Immunol. **156:**1–4.

10. **Graesser, D., S. Mahooti, and J. A. Madri.** 2000. Distinct roles for matrix metalloproteinase-2 and alpha4 integrin in autoimmune T cell extravasation and residency in brain parenchyma during experimental autoimmune encephalomyelitis. J. Neuroimmunol. **109:**121–131.
11. **Kramer, L. D., J. Li, and P. Y. Shi.** 2007. West Nile virus. Lancet Neurol. **6:**171–181.
12. **Leppert, D., E. Waubant, R. Galardy, N. W. Bunnett, and S. L. Hauser.** 1995. T cell gelatinases mediate basement membrane transmigration in vitro. J. Immunol. **154:**4379–4389.
13. **Lindsey, H. S., C. H. Calisher, and J. H. Mathews.** 1976. Serum dilution neutralization test for California group virus identification and serology. J. Clin. Microbiol. **4:**503–510.
14. **Liou, M. L., and C. Y. Hsu.** 1998. Japanese encephalitis virus is transported across the cerebral blood vessels by endocytosis in mouse brain. Cell Tissue Res. **293:**389–394.
15. **Luplertlop, N., D. Misse, D. Bray, V. Deleuze, J. P. Gonzalez, V. Leardkamolkarn, H. Yssel, and F. Veas.** 2006. Dengue-virus-infected dendritic cells trigger vascular leakage through metalloproteinase overproduction. EMBO Rep. **7:**1176–1181.
16. **Lustig, S., H. D. Danenberg, Y. Kafri, D. Kobiler, and D. Ben-Nathan.** 1992. Viral neuroinvasion and encephalitis induced by lipopolysaccharide and its mediators. J. Exp. Med. **176:**707–712.
17. **Malik, M., C. S. Bakshi, K. McCabe, S. V. Catlett, A. Shah, R. Singh, P. L. Jackson, A. Gaggar, D. W. Metzger, J. A. Melendez, J. E. Blalock, and T. J. Sellati.** 2007. Matrix metalloproteinase 9 activity enhances host susceptibility to pulmonary infection with type A and B strains of Francisella tularensis. J. Immunol. **178:**1013–1020.
18. **Martin, D. A., D. A. Murth, T. Brown, A. J. Johnson, N. Karabatsos, and J. T. Roehrig.** 2000. Standardization of immunoglobulin M capture enzyme-linked immunosorbent assays for routine diagnosis of arboviral infections. J. Clin. Microbiol. **38:**1823–1826.
19. **Morrey, J. D., A. L. Olsen, V. Siddharthan, N. E. Motter, H. Wang, B. S. Taro, D. Chen, D. Ruffner, and J. O. Hall.** 2008. Increased blood brain barrier permeability is not a primary determinant for lethality of West Nile virus infection in rodents. J. Gen. Virol. **89:**467–473.
20. **Page-McCaw, A., A. J. Ewald, and Z. Werb.** 2007. Matrix metalloproteinases and the regulation of tissue remodelling. Nat. Rev. Mol. Cell Biol. **8:**221–233.
21. **Pardridge, W. M.** 1983. Brain metabolism: a perspective from the blood-brain barrier. Physiol. Rev. **63:**1481–1535.
22. **Parks, W. C., C. L. Wilson, and Y. S. Lopez-Boado.** 2004. Matrix metalloproteinases as modulators of inflammation and innate immunity. Nat. Rev. Immunol. **4:**617–629.
23. **Rios, M., M. J. Zhang, A. Grinev, K. Srinivasan, S. Daniel, O. Wood, I. K. Hewlett, and A. I. Dayton.** 2006. Monocytes-macrophages are a potential target in human infection with West Nile virus through blood transfusion. Transfusion **46:**659–667.
24. **Romanic, A. M., and J. A. Madri.** 1994. Extracellular matrix-degrading proteinases in the nervous system. Brain Pathol. **4:**145–156.
25. **Rosenberg, G. A., E. Y. Estrada, and J. E. Dencoff.** 1998. Matrix metalloproteinases and TIMPs are associated with blood-brain barrier opening after reperfusion in rat brain. Stroke **29:**2189–2195.
26. **Rosenberg, G. A.** 2002. Matrix metalloproteinases in neuroinflammation. Glia **39:**279–291.
27. **Samuel, M. A., and M. A. Diamond.** 2006. Pathogenesis of West Nile virus infection: a balance between virulence, innate and adaptive immunity, and viral evasion. J. Virol. **80:**9349–9360.
28. **Samuel, M. A., H. Wang, V. Siddharthan, J. D. Morrey, and M. S. Diamond.** 2007. Axonal transport mediates West Nile virus entry into the central nervous system and induces acute flaccid paralysis. Proc. Natl. Acad. Sci. USA **104:**17140–17145.
29. **Sellner, J., F. Simon, U. Meyding-Lamade, and S. L. Leib.** 2006. Herpes-simplex virus encephalitis is characterized by an early MMP-9 increase and collagen type IV degradation. Brain Res. **1125:**155–162.
30. **Wang, T., T. Town, L. Alexopoulou, J. F. Anderson, E. Fikrig, and R. A. Flavell.** 2004. Toll-like receptor 3 mediates West Nile virus entry into the brain causing lethal encephalitis. Nat. Med. **10:**1366–1373.
31. **Welgus, H. G., E. J. Campbell, J. D. Cury, A. Z. Eisen, R. M. Senior, S. M. Wilhelm, and G. I. Goldberg.** 1990. Neutral metalloproteinases produced by human mononuclear phagocytes. Enzyme profile, regulation, and expression during cellular development. J. Clin. Investig. **86:**1496–1502.
32. **Yong, V. W.** 2005. Metalloproteinases: mediators of pathology and regeneration in the CNS. Nat. Rev. Neurosci. **6:**931–944.